A wireless haptic data suit for controlling humanoid robots

Alessandro Graziano, Scuola Superiore Sant'Anna, Pisa, Italy
Paolo Tripicchio
Carlo Alberto Avizzano
Emanuele Ruffaldi

Abstract

In this paper we present a novel wearable suit for haptic feedback capabilities at user's hands combined with upper body motion tracking. In the work we present both the system design and the algorithms used for motion tracking and haptic rendering. The overall system was applied to the co-located tele-operation of the Baxter research robot to perform manipulative tasks usually carried out by human personnel in the industry.

1 Introduction

In the last years major robots companies commercialized several humanoid industrial robots to allow to automate phases of industrial processes that require high dexterity and that nowadays are performed only by humans. These robots are the Baxter Robot by Rethink Robotics, the YUMI by ABB, the dual LBR by KUKA, the Dual Arm Wisematic by Epson, the Nextage by Kawada Industries. The processes that involve this category of robots are characterized by assembling and repetitive tasks not easily transferable to an automatic platform, making the robot programming not trivial. This trend caused a growing need of devices to interface with such robotic platforms and to transfer the human dexterity to them. The programming by demonstration (PbD) research field [7] is aimed at the development of algorithms and tools to program a robot simply showing it the action to perform. This method allows to subtract humans from the tedious repetitive manipulative industrial tasks like the ones usually found in the assembly lines. In some cases PbD can be performed by kinesthetically teaching the robot, or, if possible, by showing without directly interacting with it. The later approach requires to finely track the human movements and it demonstrates that a fundamental role is played by the force and impedance exerted by human operators. Within this context our paper presents a novel wearable suit to capture human movements and to provide force feedback exerted over the index-thumb fingers while performing generic bimanual manipulative tele-operation tasks [1]. Such suit meets the requirements of various research fields in terms of human body tracking and haptic feedback. The developed hardware and algorithms find application first in the programming by demostration field, but also in teleoperation applications, virtual environment interaction and all robotic fields that require to track human motor activities. The aim of the application of this technology to robot programming is to create a new category of robots able to interact with the surrounding by using strategies learned directly by the human actions. The developed suit was applied to a teleoperation/PbD task using a research robotic platform that has gained great success in the last year: the Baxter Research Robot by Rethink [4]. The overall system was tested to perform bimanual teleoperation tasks with this robot [8, 9, 10, 11]. The system offered the possibility to capture and record the way how humans perform some manipulative/assembly tasks. The collected data allowed to solve the difficult programming task generalizing first and then transferring the human dexterity to a robotic platform. We tested the system in different scenarios populated with various-stiffness objects that simulate both industrial and domestic cases. The system showed good performance in guiding the Baxter robot to perform pick and place operation with a failure rate near zero and some more complex bimanual task like passing an object from a hand to the other one.

The sections are organized as follows. In the Section 2 there is an overview of the suit, in section 3 the algorithms used for haptic rendering and attitude estimation are explained in detail, in section 4 the joint angles reconstruction and the motion mapping for tele-operation is described, in section 5 experimental results are presented.

2 Suit Description

The suit was designed to meet some important features that are difficult to find in other similar products. First, the system was designed to be fully portable and so battery-powered. To overcome the problem of different sized people we realized the suit in the form of multiple elastic strip containing the electronics, the sensors and the batteries. All the modules are WiFi and can be connected to a network infrastructure or directly to a mobile platform like a PC or a smartphone to collect the data, compute various algorithms

and send the results remotely or locally to a robotic platform. Furthermore the suit is modular, the haptic interface and the motion capture system can be used independently for different applications.

2.1 Motion Capture System

The motion capture system is made of several 9-axis Inertial Motion Unit (IMU) sensors mounted on arms, forearms, hands and torso of the users, and it is capable to capture the upper-body human movements in terms of joint angles of a kinematic tree describing the human kinematic structure or simply in terms of the position of the hands with respect to the torso [2].

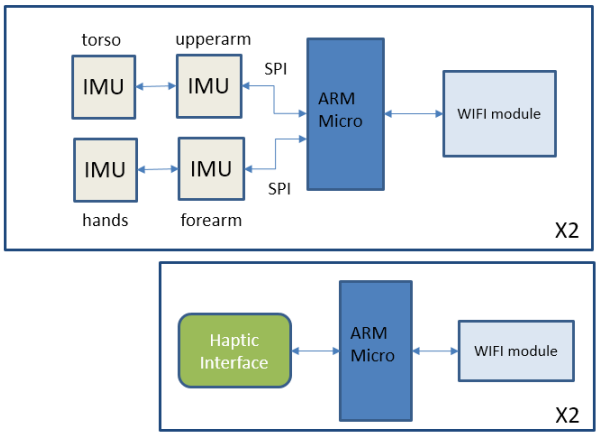

Figure 1 Suit Architecture Diagram showing the inertial capture for each arm on the top part, and the haptic feedback on the bottom part.

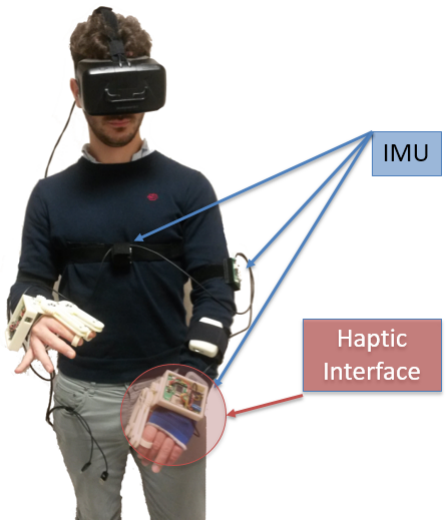

Figure 2 Real wearable suit in which the user is wearing an Oculus HMD for telepresence

The IMU sensors used in this work are the InvenSense 9250 set with the features described in table 1.

Gyro Full Scale Range	$\pm 250 \, \mathrm{deg}/s$
Gyro Rate Noise	$0.01 \frac{\mathrm{deg}/s}{\sqrt{Hz}}$
Accel Full Scale Range	$\pm 2g$
Compass Sensitivity	$0.6 \mu T / LSB(14-bit)$
Digital Interface	SPI

Table 1 Invensense 9250 features

2.1.1 Custom Board

To read the sensor data and to send them to a computer we developed a board made up of three main components:

- An IMU sensor InvenSense 9250 described above.
- A WIFI IoT module to stream the data.
- A Microcontroller ARM Cortex M4 STM32F407 running at 168MHz to read the IMU sensor with the SPI protocol and to send the collected data to the WIFI module with the USART protocol.

Such board is versatile because it can be used also to control the haptic interface. In fact additional connectors were added to read an incremental encoder, to read an analog signal and to send a PWM signal to a driver of a DC motor. In figure 3 the board is illustrated.

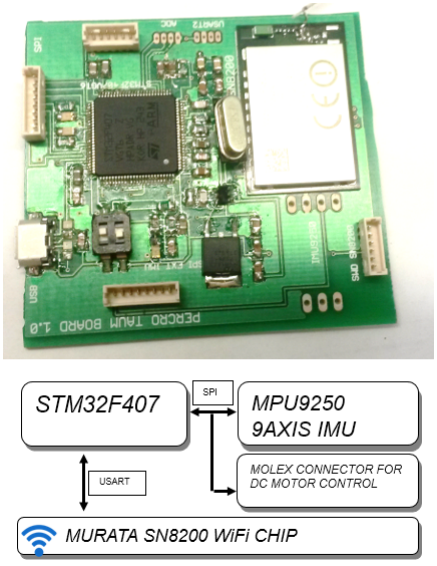

Figure 3 Custom Board

2.2 Haptic Interface

The purpose of the haptic interface is to allow the user to manipulate object with a teleoperated robotic arm.
Many industrial and research robotic platforms make use of a simplified 1 degree of freedom (DOF) gripper as end-effector to be able to grasp objects. For such a reason we focused on the development of 1 DOF haptic interface in order to correctly drive the robotic gripper counterpart.

The chosen correspondence for the user motion is the human pinch movement. This movement is characterized by a coupled motion of the index and thumb fingers in order to effect a force-closure in the grasp given by the contact between the human(or robotic) fingers and two surfaces of the manipulated object.
The haptic interface was designed in multiple steps by using the power and the speed of the rapid-prototyping offered by the 3D printing. We realized two version of such hand-mounted device: the first one was built with a in-extensible cable-based transmission, the second one instead was realized with a gear-based transmission. Both the version of the haptic interface are actuated with a highly reduced micromotor (300:1) equipped with a magnetic encoder. The haptic rendering was tested first by interacting with virtual objects [1, 12] and then it has been tested with a Rethink Robotics Baxter robot. Both the robotic platforms have 1 DOF gripper that is controlled in position. This is due to the fact that this kind of gripper has a reduced velocity to not brake the grasped object but obviously this introduces a delay in the teleoperation loop. To overcome this problem and maintain loop stability a virtual coupling haptic rendering algorithm was implemented.

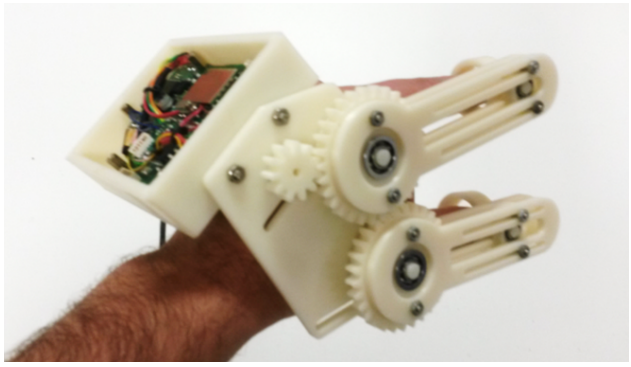

Figure 4 Haptic Interface with gear transmission

3 Algorithms description

In this section we describe the algorithms used for motion reconstruction and for haptic rendering. First let introduce the notation and the human arm kinematic model employed in this work. A 7 DoF kinematic chain was used to model each human arm. Three DoF model the shoulder, two DoF the elbow and two DoF the wrist. We report here the DH table used for left arm in table 2. The parameters l_{fa} and l_{ua} indicating respectively the length of the upperarm and the forearm are manually measured and set in the model.

Frame	a_i	α_i	d_i	θ_i
1	0	$\frac{\pi}{2}$	0	$\theta_1 + \frac{\pi}{2}$
2	0	$\frac{\pi}{2}$	0	$\theta_2 - \frac{\pi}{2}$
3	l_{ua}	0	0	$\theta_3 + \frac{\pi}{2}$
4	0	$\frac{\pi}{2}$	0	$\theta_4 + \frac{\pi}{2}$
5	0	$\frac{\pi}{2}$	l_{fa}	$\theta_5 + \frac{\pi}{2}$
6	0	$\frac{\pi}{2}$	0	$\theta_6 + \frac{\pi}{2}$
7	0	0	0	θ_7

Table 2 DH table of the human arm model

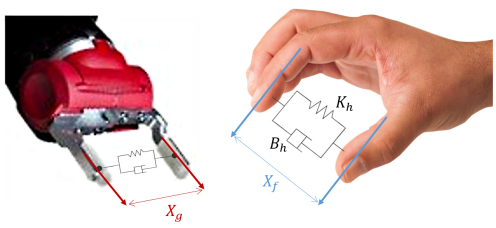

Figure 5 Schematics of the haptic feedback and correlation between user hand and robot gripper(in the picture the Baxter gripper)

In figure 6 a schematics of the frames used for the left arm is illustrated. Notice that there are four additional frames indicating the inertial sensors: these are S_T, S_U, S_F and S_H respectively for the sensors attached to torso, upperarm, forearm and hand. Let name S_i the i-th frame of the DH kinematic chain, we suppose that S_T is rigidly attached to S_1, S_U to S_3, S_F to S_5 and S_H to S_8. Our algorithm aims at calculating the joint angles and the end-effector position of the kinematic chain described above by estimating the relative attitudes of the sensor frames.

3.1 Attitude Estimation

The attitude estimation of the sensor frame is done by using a filter similar to the one presented in [5]. Such filter allows to estimate the inertial sensor orientation with respect to the a earth-fixed frame named S_E measuring the acceleration, the angular velocity and the magnetic field: First, the filter estimates the orientation by integrating the angular rate measured by the gyroscope, employing the classical quaternion representation. The integration equations are:

$$ {}^S_E q_{\omega,t} = {}^S_E \hat{q}_{est,(t-1)} + {}^S_E \dot{q}_{(\omega,t)} \Delta \tag{1} $$

$$ {}^S_E \dot{q}_{\omega,t} = \frac{1}{2} {}^S_E \hat{q}_{est,(t-1)} \otimes {}^S \omega_t \tag{2} $$

where ${}^S_E q_{\omega,t}$ indicates the quaternion describing the rotation between the frame S_E and S_S, with S_S indicating a sensor attached frame. The subscript $_\omega$ indicates that the estimation is done with the angular velocity measure only. ${}^S\omega$ denotes the angular velocity expressed in the frame S_S. Δ is the integration step.
The filter uses also the accelerometer and magnetometer measures to estimate the orientation and to overcome the

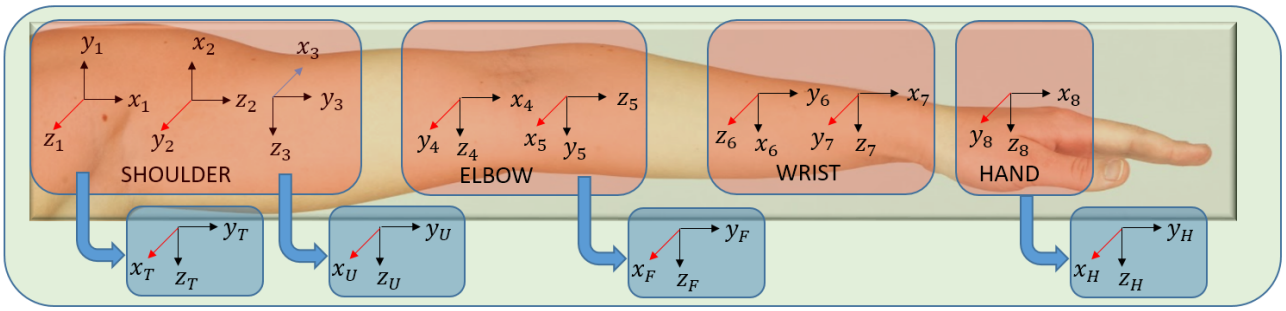

Figure 6 Schematics of the frames used in the kinematic model

drifting problems. The estimation is formulated as an optimal problem.
The objective function is:

$$f\left({}^{S}_{E}q, {}^{E}d, {}^{S}r\right) = {}^{S}_{E}q^{*} \otimes {}^{E}d \otimes {}^{S}_{E}q - {}^{S}r \tag{3}$$

with

$${}^{S}r = \begin{bmatrix} {}^{S}a \\ {}^{S}m \end{bmatrix}, {}^{E}d = \begin{bmatrix} 0 \\ 0 \\ 1 \\ 1 \\ 0 \\ 0 \end{bmatrix} \tag{4}$$

${}^{E}d$ indicates the acceleration and magnetic field expected components in the S_E frame. Notice that such components are for NWU North-West-Up reference frame. Employing the gradient descent method to minimize the function in (3), the algorithm results as follows:

$${}^{S}_{E}q_{\nabla,t} = {}^{S}_{E}q_{est,(t-1)} - \mu \frac{\nabla f\left({}^{S}_{E}q, {}^{E}d, {}^{S}r\right)}{\|\nabla f\left({}^{S}_{E}q, {}^{E}d, {}^{S}r\right)\|} \tag{5}$$

where the subscript ∇ in ${}^{S}_{E}q_{\nabla,t}$ indicates that the estimation is performed using the accelerometer and compass only. The complete estimation algorithm is:

$${}^{S}_{W}q_{est,t} = \gamma {}^{S}_{W}q_{\nabla,t} + (1-\gamma) {}^{S}_{W}q_{(\omega,t)} \tag{6}$$

where γ is a constant scalar value.

3.1.1 Compass Calibration

An important issue of the IMU attitude estimation process concerns the need of magnetometer calibration due to soft and hard-iron distortions [6]. The state of the art attitude estimation algorithms assume the magnetometers to be calibrated before starting the filtering process. This is usually performed by collecting measures of the magnetic field while moving the sensor around three orthogonal circumferences and then finding the parameters of a 3D ellipsoid fitted on the collected data. In fact, varying the orientation of the sensor, the collected measures of the magnetic field in general belong to a generic ellipsoid while they must belong to a sphere centered in the origin. The main drawback of such approach is that the magnetometer calibration parameters can change if the sensor position is too far from the place where the calibration was performed. Furthermore the calibration parameters can change with the time if, for example, other devices are powered up or off nearby the sensor or the sensor approaches some sources of electromagnetic interference. To model the distortion errors an affine function can be used:

$${}^{S}\hat{m} = T_S {}^{S}m + {}^{S}c \tag{7}$$

where ${}^{S}\hat{m}$ is the distorted magnetic field in component with respect to the sensor fixed reference frame and

$$A_s = \begin{bmatrix} \alpha & 0 & 0 \\ 0 & \beta & 0 \\ 0 & 0 & \gamma \end{bmatrix}, {}^{S}c = \begin{bmatrix} {}^{S}_{x}c \\ {}^{S}_{y}c \\ {}^{S}_{z}c \end{bmatrix} \tag{8}$$

Finding the right values for the terms A_S and ${}^{S}c$ in (7) is the aim of the calibration procedure. Such terms are usually found by fitting an ellipsoid to a set of data collected while moving randomly the sensor in a way to explore uniformly all the direction. As announced above, the calibration is usually performed once in batch before starting to use the magnetometer, for this reason it suffers the problem that the sensor must remain in the neighborhood of the place where the calibration was made because of the variability of the magnetic field. To overcome this limitation we propose a recursive calibration scheme that continuously estimates the calibration parameters. The employed sensor provides the term A_S by default so the calibration objective is to find the components of ${}^{S}c$.
The iterative calibration scheme is based on a Kalman filter, where the state update model is without noise:

$$x_{k+1} = x_k, \; x = \begin{bmatrix} {}^{S}_{x}c \\ {}^{S}_{y}c \\ {}^{S}_{z}c \end{bmatrix} \tag{9}$$

The measurement model is the simple equation of a sphere:

$$y_k = Cx_k + \varepsilon = 0 =$$

$$= \begin{pmatrix} {}^S_x m^2 + {}^S_y m^2 + {}^S_z m^2 & -2{}^S_x m & -2{}^S_y m & -2{}^S_z m & 1 \end{pmatrix} \begin{pmatrix} 1 \\ {}^S_x c_k \\ {}^S_y c_k \\ {}^S_z c_k \\ R^2 \end{pmatrix} + \varepsilon \tag{10}$$

where ${}^S_x m$, ${}^S_y m$, and ${}^S_z m$ are the components of the compass measures in the sensor frame. The estimation equations are:

$$x^-_{k+1} = x^-_k \tag{11}$$

$$x^+_{k+1} = x^+_k + L(0 - Cx^-_k) \tag{12}$$

With

$$L = Q_k C \left(C^T Q_k C + R\right)^{-1} \tag{13}$$

$$Q_{k+1} = Q_k - LC^T Q_k \tag{14}$$

where Q is the covariance matrix of the state estimate. The matrix R is the covariance of the measurement noise. While usually the matrix R is set to a constant value, we defined a policy to set the matrix R according to the angular velocity of the sensor measured by the gyroscope in a way to give more relevance to the measures taken with a higher angular velocity. This technique was adopted to avoid to accumulate relevant measures when the sensor is not moving. In particular R was set to:

$$R = \begin{cases} \frac{1}{\|\omega\|}, & \text{if } \|\omega\| < l \\ \frac{1}{l}, & \text{otherwise} \end{cases} \tag{15}$$

where l is a constant threshold.

3.2 Sensor Orientation Calibration

As we said above we rigidly attached four IMU to the body, one to the torso, one to the upperarm, one to the forearm and one to the hand. Inevitably the wearing phase introduces some little uncertainties in the orientation of the sensors with respect to the body parts.

As described at the beginning of this section the sensors are supposed to be rigidly attached to the frame S_1, S_3, S_5 and S_8 of the kinematic chain.

To estimate the right orientation of the inertial sensors with respect to the DH frames we set a calibration procedure requiring the user to stay in three different poses as illustrated in figure 7 (These figures have been created interfacing the suit with the Unity 3D Game Engine). The algorithm collects measures of the sensors attitude in these three different poses and then with an optimization algorithm it finds the poses of the sensors with respect to the frames of the kinematic chain.

In particular for each sensor we obtain three sets of m measured poses and three sets of m target poses. The orientations of the sensors are set to the solution of this optimal problem:

$${}^A_B\hat{q} = \min_{{}^A_B q} \sum_{j=1}^{m} \sum_{k=1}^{3} \left\| {}^A_E q_k - {}^A_B q \, {}^B_E q_{est,j,k} \right\| \tag{16}$$

with $(A,B) \in \{\{S_T, S_1\}\{S_U, S_3\}\{S_F, S_5\}\{S_H, S_8\}\}$

3.3 Haptic Rendering

Figure 5 shows the variables used by the haptic rendering algorithm. X_f is the distance between the index and thumb fingers measured by means of a magnetic encoder attached to the DC motor shaft and the haptic device direct kinematic parameters. X_g is the distance between the gripper fingers. K_h and B_h are the parameters of the haptic impedance feedback exerted at the user fingers. The final haptic rendering algorithm becomes:

$$F = -K_h(X_f - X_g) - B_h(\dot{X}_f - \dot{X}_g) \tag{17}$$

The same algorithm is used back to compute the new X_g position reference for the robotic griper.

4 Joint Angles Estimation

The information obtained with the attitude estimation filter is used to recover the human arm kinematic state by employing an inverse kinematics algorithm using the knowledge of the human kinematic structure.

To estimate the joint angles of such kinematic tree we used an inverse kinematics algorithm. In particular using the estimates of the attitude of each sensor frame obtained from the inertial measures, the algorithm uses the closed form inverse kinematics function available for the employed kinematic structure.

In particular the decoupled orientation estimation of the IMU sensors provide us an estimation of the relative attitude between the respective attached frames of the kinematic chain as described in section 3. So let be ${}^T_E q$, ${}^U_E q$, ${}^F_E q$, ${}^H_E q$ respectively the attitute of the Torso, the Upperarm, the Forearm and the Hand with respect to the NWU reference frame. We can obtain the relative attitudes ${}^T_U q$, ${}^U_F q$, ${}^F_H q$ simply combining the previous ones. Then it is trivial to extract the joint angles. In fact, with reference to the kinematic structure described in table 2 and illustrated in figure 6, ${}^T_U q$ is a function of $\theta_1, \theta_2, \theta_3$, ${}^U_F q$ is a function of θ_4, θ_5 and ${}^F_H q$ of θ_6, θ_7

4.1 Motion mapping

To teleoperate the Baxter Robot an end-effector kinematic mapping scheme was adopted. In particular let x_H be the estimated human hand pose with respect to the human torso and x_R the robot end-effector position, furthermore let assume that the transformation between the robotic torso and end-effector be congruent with the transformation between

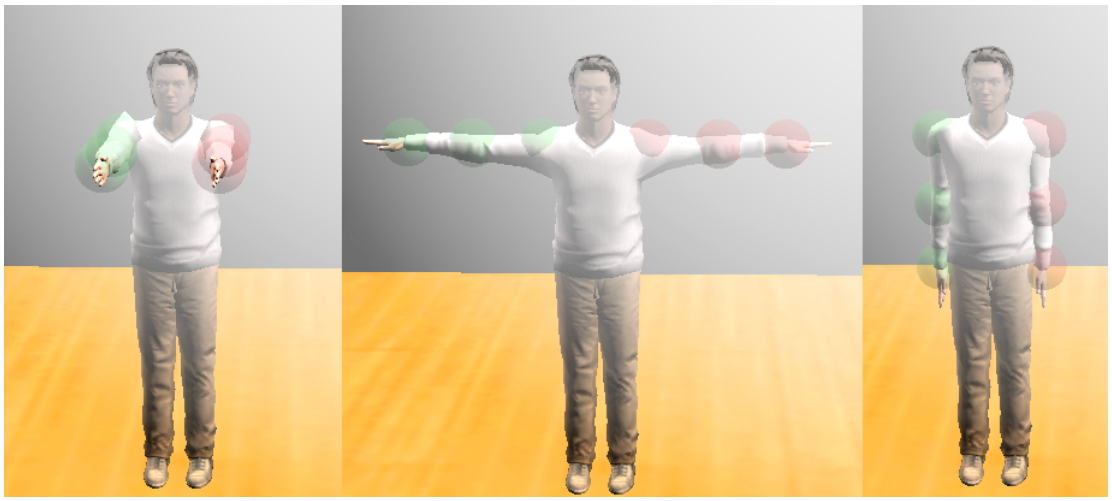

Figure 7 Calibration poses

the human torso and hand, then the robotic arm is controlled to minimize the quantity $e = \|x_H - x_R\|$.
A closed loop inverse kinematic scheme (CLIK) with the pseudo-inverse of the robot end effector jacobian matrix was adopted.

$$q_{R,k+1} = q_{R,k} + J^{+}\left(x_{H,k} - x_{R,k}\right) \tag{18}$$

where J^{+} indicates the pseudoinverse of robot jacobian matrix. To obtain a real-time inverse kinematics we perform only three step of such iterative equation for each new estimated hand pose.

5 Experimental Results

We validated the motion reconstruction system with an high precision optical tracking system (TRIO system by OptiTrack). We report the temporal evolution of the hand position estimated with our algorithm and the respective optical measures in figures 9-11. Figure 12 shows that the maximum reconstruction error is less than 2 cm.
We report the results of two experiments performed with the suit in a teleoperation scenario. Figure 8 illustrates a schematic of such scenario. In the first experiment the user teleoperates the Baxter robot performing a circular movement with the hand.
The human hand position and the robot end effector position are shown in figure 13. Notice that the teleoperation error is due substantially to a delay caused by the position control system of the robot arm. The other test performed is a pick and place teleoperation task: a user guides the robot with the full suit to grasp a three diferrent objects and put them in a target place. The objects are: a tennis ball, a little plastic bottle and a glass. The distance between the source and target places is 50cm. The task is considered completed if the user moves the objects to the target place with a maximum error of 5cm. Table 3 reports the results of such experiment:

N. of tests	30
Completion time Mean	67.4s
Completion time Standard Deviation	18.3s
Success Rate	100%

Table 3 Results of the pick and place teleoperation

6 Future Work

In this paper we presented the hardware and software design of an integrated suit for motion capture and haptic feedback. Future developments include:

- Improve the reconstruction accuracy and the human-robot kinematic mapping using statistical information on human movements.
- Improve the haptic response developing other haptic rendering algorithms.
- Design of an algorithm for the automatic estimation of the human limbs lengths.

7 Literature

[1] Bergamasco, Massimo, et al. "Design and validation of a complete haptic system for manipulative tasks." Advanced Robotics 20.3 (2006): 367-389.

[2] Peppoloni, Lorenzo, et al. "A novel 7 degrees of freedom model for upper limb kinematic reconstruction based on wearable sensors." Intelligent Systems and Informatics (SISY), 2013 IEEE 11th International Symposium on. IEEE, 2013.

[3] Peppoloni, L., et al. "A novel wearable system for the online assessment of risk for biomechanical load in repetitive efforts." International Journal of Industrial Ergonomics 52 (2016): 1-11.

[4] Ju, Zhangfeng, Chenguang Yang, and Hongbin Ma. "Kinematics modeling and experimental verification

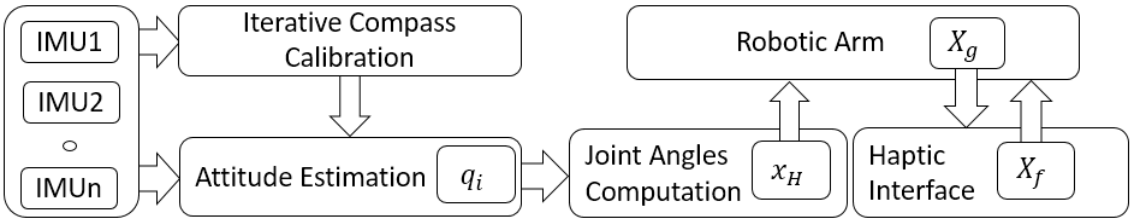

Figure 8 Schematic of the teleoperation scenario

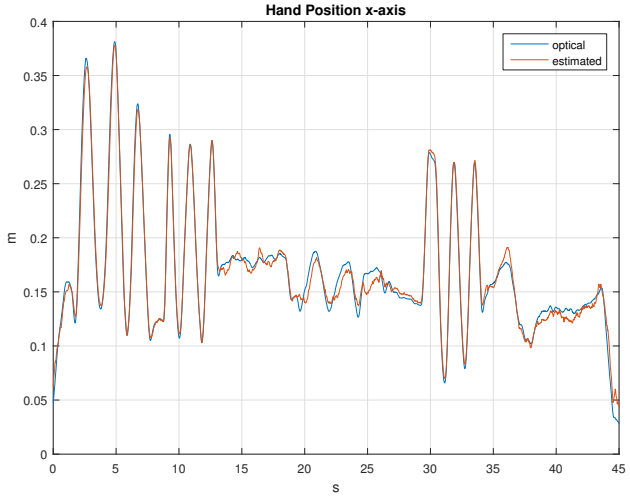

Figure 9 Comparison of the estimated hand position with the high precision optical system data x axis

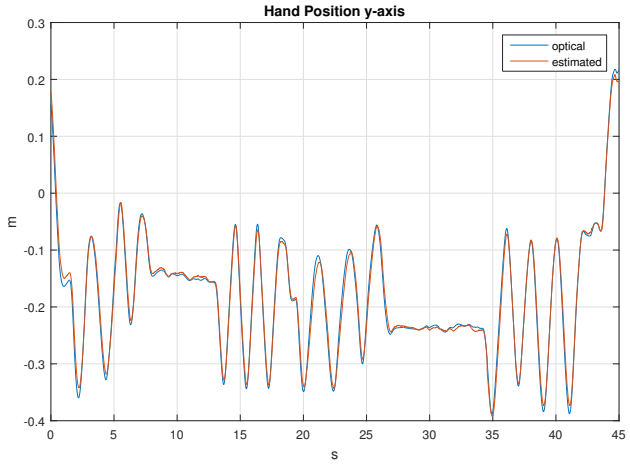

Figure 10 Comparison of the estimated hand position with the high precision optical system data y axis

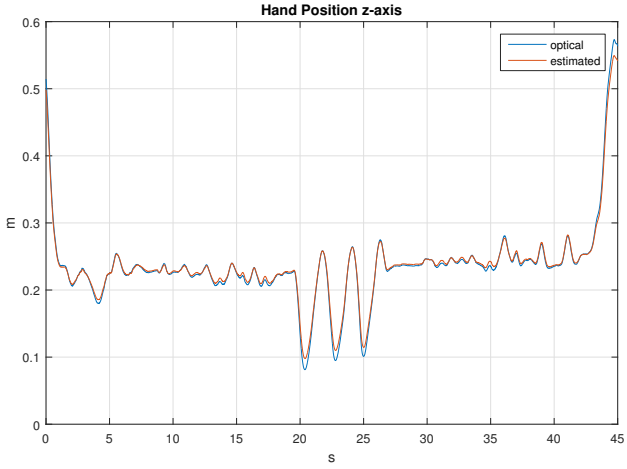

Figure 11 Comparison of the estimated hand position with the high precision optical system data z axis

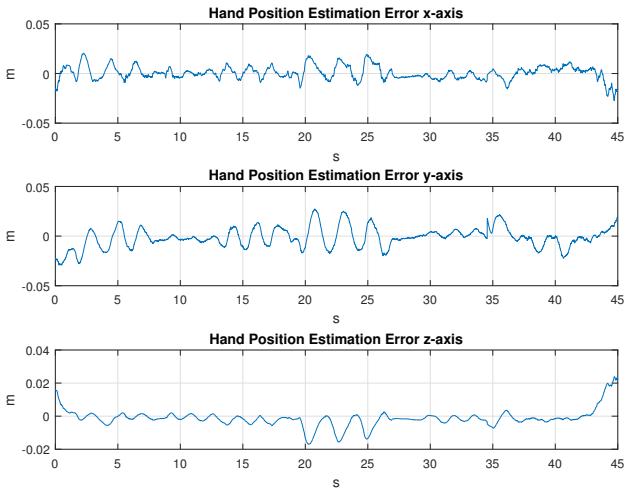

Figure 12 Estimation Error

of baxter robot." Control Conference (CCC), 2014 33rd Chinese. IEEE, 2014.

[5] Madgwick, Sebastian OH, Andrew JL Harrison, and Ravi Vaidyanathan. "Estimation of IMU and MARG orientation using a gradient descent algorithm."Rehabilitation Robotics (ICORR), 2011 IEEE International Conference on. IEEE, 2011.

[6] Dorveaux, Eric, et al. "Iterative calibration method for inertial and magnetic sensors." Decision and Control, 2009 held jointly with the 2009 28th Chinese Control Conference. CDC/CCC 2009. Proceedings of the 48th IEEE Conference on. IEEE, 2009.

[7] Billard, Aude, et al. "Robot programming by demonstration." Springer handbook of robotics. Springer

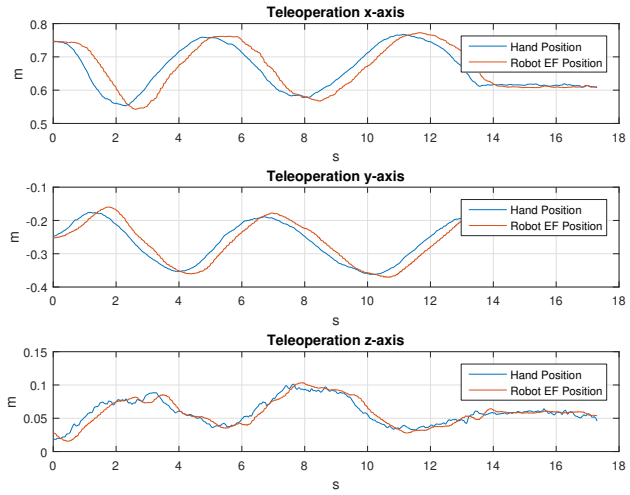

Figure 13 Position coordinates during a teleoperation

Berlin Heidelberg, 2008. 1371-1394.

[8] Ha, ChangSu, et al. "Whole-body multi-modal semi-autonomous teleoperation of mobile manipulator systems." Robotics and Automation (ICRA), 2015 IEEE International Conference on. IEEE, 2015.

[9] Miller, Nathan, et al. "Motion capture from inertial sensing for untethered humanoid teleoperation." Humanoid Robots, 2004 4th IEEE/RAS International Conference on. Vol. 2. IEEE, 2004.

[10] Seo, Yongho, Heonyoung Park, and Hyun Seung Yang. "Wearable Telepresence System using Multimodal Communication with Humanoid Robot." ICAT. 2003.

[11] Fritsche, Lars, et al. "First-person tele-operation of a humanoid robot."Humanoid Robots (Humanoids), 2015 IEEE-RAS 15th International Conference on. IEEE, 2015.

[12] Ang, Quan-Zen, et al. "Enabling multi-point haptic grasping in virtual environments." 3D User Interfaces (3DUI), 2011 IEEE Symposium on. IEEE, 2011.

[13] Pierce, Rebecca M., Elizabeth Fedalei, and Katherine J. Kuchenbecker. "A wearable device for controlling a robot gripper with fingertip contact, pressure, vibrotactile, and grip force feedback." Haptics Symposium (HAPTICS), 2014 IEEE. IEEE, 2014.

[14] Bischoff, Rainer, Ulrich Huggenberger, and Erwin Prassler. "Kuka youbot-a mobile manipulator for research and education." Robotics and Automation (ICRA), 2011 IEEE International Conference on. IEEE, 2011.